Journal of Materials Chemistry A

PAPER

View Article Online
View Journal | View Issue

Cite this: J. Mater. Chem. A, 2014, 2, 3841

Stable wire-shaped dye-sensitized solar cells based on eutectic melts†

Houpu Li, Zhibin Yang, Longbin Qiu, Xin Fang, Hao Sun, Peining Chen, Shaowu Pan and Huisheng Peng*

Received 16th September 2013
Accepted 12th December 2013

DOI: 10.1039/c3ta13714g

www.rsc.org/MaterialsA

Wire-shaped dye-sensitized solar cells (DSCs) have recently attracted increasing interest due to their unique and promising advantages, such as being lightweight, deformable and weavable compared to conventional planar structures. However, the use of liquid electrolytes based on organic solvents has largely limited their practical applications, *e.g.*, low mechanical and thermal stabilities. Solid-state electrolytes are resistive to these problems in nature, and have been shown to have high stability. Herein, eutectic melts, for the first time, have been introduced as the electrolyte to develop novel wire-shaped DSCs. The resulting wire-shaped DSCs were flexible and highly stable thermally and their energy conversion efficiencies could recover entirely after heating up to 110 °C.

Introduction

It is not an exaggeration to say that the world will endure a global energy crisis in the near future. The foreseeable exhaustion of fossil fuels has boosted the development of alternative energy sources. As one of the promising candidates, solar power has hitherto attracted massive amounts of attention and thus inspired the exploitation of photovoltaic devices.[1] The traditional silicon-based technology has confronted serious challenges as the heavy bulky packages are impractical for the ever-growing requirements of portable, flexible and low-cost devices.

Emerging in the 1990s, dye-sensitized solar cells (DSCs) have matured and flourished considerably over the last decade.[2] Nevertheless, the conventional planar structure may still limit their application in the upsurging fields of weavable and stretchable photovoltaic devices.[3] To this end, novel wire-shaped DSCs were proposed and typically fabricated by intertwining two fiber electrodes together to form a wire-shaped structure.[4–8] For a typical fabrication, the intertwined fiber electrodes are first inserted into a transparent tube, followed by injecting the liquid electrolytes with organic solvents and sealing at two ends.[9] The liquid electrolytes with organic solvents suffer from leakage and low stability during use, which is unfavourable for broad applications.[10] The required bending or other deformations in portable electronic devices make the problem even more severe. Therefore, improvement of the stability is critically important for the wire-shaped DSC.

Ionic liquids have been widely studied for various electronic devices due to their high ionic conductivities and wide electrochemical windows.[11] In addition, they show a near-to-zero vapor pressure, and are therefore immune to the problem of vaporization. The combined remarkable electrochemical and thermal properties make them suitable for promising applications in DSCs.[12,13] Due to specific pendant groups such as ethyl and regular structures, the ionic liquids that are solid at room temperature are named ionic liquid crystals.[14] Such ionic liquid crystals are expected to replace the conventional liquid electrolytes to obviate the longstanding leakage problem.[10,15] These ionic liquids, particularly ionic liquid crystals, may also represent a general and effective strategy to resolve the remaining problems of wire-shaped DSCs, although no reports are available in this field.

Herein, to the best of our knowledge, we first report a novel wire-shaped DSC based on eutectic melts, a mixture of ionic liquid crystal and ionic liquid, as electrolytes. The resulting wire-shaped DSCs are flexible, highly stable thermally and have energy conversion efficiencies that can entirely recover after heating up to 110 °C.

Experimental section

(1) Synthesis of 1-ethyl-3-methylimidazolium iodide (EMII)

The ionic liquid crystal, EMII, was synthesized according to the following procedure.[16] In a three-necked flask purged with nitrogen, 0.1 mol (7.97 mL) 1-methylimidazole was dissolved in 15 mL of acetonitrile, and 0.1 mol (8.08 mL) ethyl iodide was then added dropwise under vigorous stirring over 1 h. The mixture was stirred for another 24 h at room temperature, followed by adding 100 mL ethyl acetate under vigorous stirring. White crystals were precipitated immediately. The resulting

State Key Laboratory of Molecular Engineering of Polymers, Department of Macromolecular Science, Laboratory of Advanced Materials, Fudan University, Shanghai 200438, China. E-mail: penghs@fudan.edu.cn

† Electronic supplementary information (ESI) available. See DOI: 10.1039/c3ta13714g

product was collected by filtering membranes, and then washed with ethyl acetate and diethyl ether, for three times each. The yield was ~70%. The product was characterized by H^1-NMR (δ/ppm): 1.56 (t, 3H), 4.10 (s, 3H), 4.46 (q, 2H), 7.85 (br d, 2H), 9.68 (s, 1H).

(2) Synthesis of 1-propyl-3-methylimidazolium iodide (PMII)

The synthesis of PMII was similar to that of EMII.[16] In a three-necked flask purged with nitrogen, 0.1 mol (7.97 mL) 1-methylimidazole was dissolved in 15 mL isopropanol, and 0.1 mol (9.71 mL) propyl iodide was then added dropwise with vigorous stirring over 1 h. The mixture was then stirred for another 24 h at 80 °C and cooled down to room temperature, followed by washing with ethyl acetate and diethyl ether, for three times each. The solvent was vaporized and the product was dried under vacuum for three days with a yield of ~70%. The resulting product was also characterized by H^1-NMR (δ/ppm): 0.94 (t, 3H), 1.97 (sx, 2H), 4.10 (s, 3H), 4.40 (q, 2H), 7.90 (br d, 2H), 9.69 (s, 1H).

(3) Preparation of eutectic melts

Different ratios of PMII and iodine in the electrolyte leads to different ratios of I^- and I_3^-, thus affecting the energy level of the electrolyte, which, in the end, leads to a trade-off between the voltage and current density for the solar cell.[17] In this work, we chose an optimized ratio of 24/1 according to the literature.[18] Ionic liquid PMII (6.05 g, 24 mmol) and iodine (0.254 g, 1 mmol) were mixed and dissolved in acetonitrile in a 10 mL volumetric flask, obtaining a mixture with a PMII–iodine mole ratio of 24/1. 1 g of EMII and a certain amount of PMII–iodine solution (*e.g.*, 0.158 mL for 10%, 0.237 mL for 15%, *etc.*) were mixed and ultrasonically treated for 30 min. The mixture was stirred for 8 h and then heated to 80 °C overnight, followed by drying in vacuum to remove the acetonitrile. The eutectic melts appeared dark purple in colour.

(4) Preparation of working electrodes

The working electrode has been previously reported.[7] To summarize, titanium wires (Alfa-Aesar, diameter of 0.005 inch and purity of 99.9%) were anodized in an ethylene glycol solution containing 0.3 wt% NH_4F and 8 wt% H_2O at a bias voltage of 60 V. The anodized titanium wire was then annealed at 500 °C in air for 60 min. After that, the annealed titanium wire was treated by 100 mM $TiCl_4$ solution and annealed again at 450 °C in air for 30 min to increase the roughness of the TiO_2 surface. Subsequently, the working electrode was heated to 80 °C after the second annealing and then soaked in 0.3 mM N719 solution in a solvent mixture of dehydrated acetonitrile and *tert*-butanol (volume ratio of 1/1) for 12 h to absorb dye.

(5) Preparation of fiber electrodes

Platinum (Pt) wires with a diameter of 25 μm (Alfa-Aesar, purity 99.95% Metals Basis) were used without treatment. Carbon nanotube (CNT) yarns with an average diameter of 20 μm were dry-drawn from spinnable CNT arrays which had been synthesized by chemical vapor deposition.[19] The required electrode was then prepared by twisting five CNT yarns into a larger fiber with a diameter of 45 μm. Platinum nanoparticles were deposited onto the CNT yarns by an electrochemical process.[20] To achieve a high load of platinum nanoparticles on the CNT substrate, twenty repeated deposition steps (double potential step chronoamperometry) were generally used.

(6) Characterization

H^1-NMR spectra were obtained from a Varian Mercury plus 400 MHz NMR spectrometer with acetone-D6 as the solvent. The structures were characterized by scanning electron microscopy (Hitachi FE-SEM S-4800 operated at 1 kV). The conductivities were measured in a cell that had been made from two fluorine-doped tin oxide glasses and a Surlyn film with a thickness of 60 μm (DHS-SN1760). A cuboid space with both a length and width of 5 mm and a thickness of 60 μm was formed in the cell. The melted electrolyte at 120 °C was injected into the cuboid cell through an ultrasound-drilled pinhole in one fluorine-doped tin oxide glass. The transmittances were measured based on these cuboid cells by a SHIMADZU UV-vis spectrophotometer (UV-2550). Thermal analysis was performed on a TA DSC Q2000 differential scanning calorimeter at a heating rate of 10 °C min^{-1} in a temperature range of −50 to 150 °C in a N_2 atmosphere. Optical micrographs were taken by an Olympus BX51 microscope with a DP72 image capturer. *J–V* curves were produced by a Keithley 2400 Source Meter under illumination (100 mW cm^{-2}) of simulated AM1.5 solar light generated from a solar simulator (Oriel-Sol3A 94023A equipped with a 450 W Xe lamp and an AM1.5 filter). The light intensity was calibrated using a reference Si solar cell (Oriel-91150). The energy conversion efficiencies were calculated by multiplying the length and diameter of the working electrode to be comparable with the available reports based on the same conditions.[3–5,9,20,21] For the used mask that had the same length with a width that was larger by 50% compared with the wire-shaped DSC, the efficiencies may be overestimated by 33%. The effective areas of the wire-shaped DSCs were calculated by multiplying the exposed length and diameter of the working electrodes, which is a generally accepted method.[3–5,9,20,21]

Results and discussion

The eutectic melts were prepared by mixing ionic liquid crystals of EMII with an amount of ionic liquid of PMII and iodine (Scheme 1). Here EMII offers the ionic conductivity while PMII

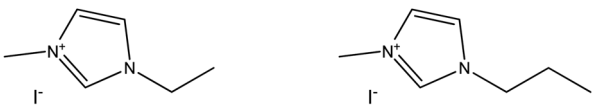

1-Ethyl-3-methyl imidazolium iodide (EMII) 1-Propyl-3-methyl imidazolium iodide (PMII)

Scheme 1 Chemical structures of 1-ethyl-3-methyl imidazolium iodide (EMII, left) and 1-propyl-3-methyl imidazolium iodide (PMII, right).

provides iodide anions (I^-) for the redox couple, and iodine generates triiodide ions (I_3^-) through reaction with iodide anions. During the preparation of the eutectic melts, PMII and iodine were previously mixed with a molar ratio of 24/1,[18] and the resulting PMII–iodine mixture was then added to the EMII to form a uniform mixture. A series of eutectic melts could be produced by varying the PMII–iodine weight percentage in the final mixture. Note that the molar ratio of PMII to iodine was maintained as 24/1. The eutectic melts remained solid when the PMII–iodine weight percentage was less than 40% and became liquid at 40% or higher (Fig. 1).

Thermal analysis was carried out to compare the solid eutectic melts with different PMII–iodine weight percentages (Fig. 2). As indicated, the melting point was 80 °C for pure EMII. When adding the PMII–iodine mixture, the melting points gradually decreased. For example, 75 °C for 10 wt% of PMII–iodine and 60 °C for a higher weight percentage of 35%. The peak sizes also lessened with the increasing PMII–iodine mixture, meaning the added doping materials undermined the EMII crystallization. As expected, no peak was observed for the eutectic melts at the critical weight percentage of 40% when they became liquids. Fig. 3 shows the optical micrographs of the eutectic melts with different PMII–iodine weight percentages. It is evident that the crystalline grains got smaller when more PMII–iodine components were introduced, suggesting the added PMII–iodine components as ion providers largely reduced sizes of the crystalline grains, which was consistent with the results in Fig. 2. The size changes of the crystalline grains were not obvious at higher weight percentages beyond 25%.

Fig. S1† shows the optical transmittances of pure EMII and the eutectic melts with different PMII–iodine weight percentages. The pure EMII showed a relatively low transmittance suggesting a very strong scattering effect ascribed to the crystallization. The transmittance of 1 M EMII solution in acetonitrile was nearly 100%, while the solid EMII was only 40%. When adding the PMII–iodine mixture, the transmittances decreased in the first place and then slightly increased, but the transmittances were all lower than 40% in the wavelength range of 500 to 800 nm, where there should be no absorption for any component of the electrolyte. The loss in the transmittances should hence be attributed to the scattering effect of crystalline grains in the electrolytes. For the eutectic melts with 20 wt% PMII–iodine, the lowest transmittance was observed, indicating the strongest scattering effect that was favorable for the light harvest in DSCs.[22] For the eutectic melts containing other weight percentages of PMII–iodine, the resulting crystalline grains were either too large or small, which diminished the scattering effect.

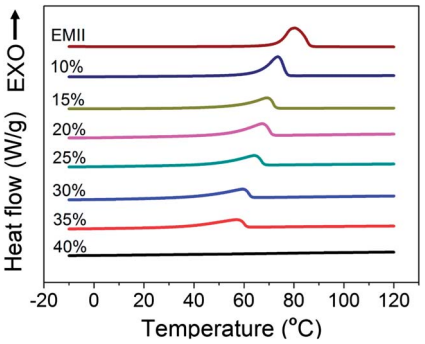

Fig. 2 Thermal analysis of EMII before and after addition of the PMII–iodine mixture with increasing the weight percentage. The number above the line corresponds to the weight percentage.

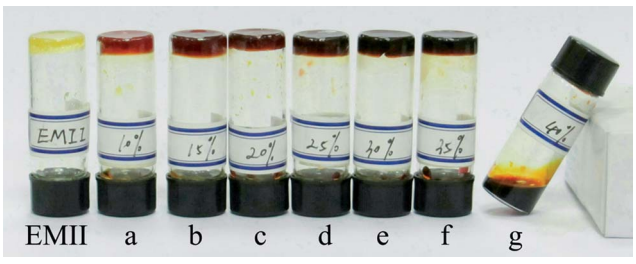

Fig. 1 Photographs of pure EMII and eutectic melts with increasing PMII–iodine weight percentages from 10% to 40%. The labeled number on the container corresponds to the weight percentage.

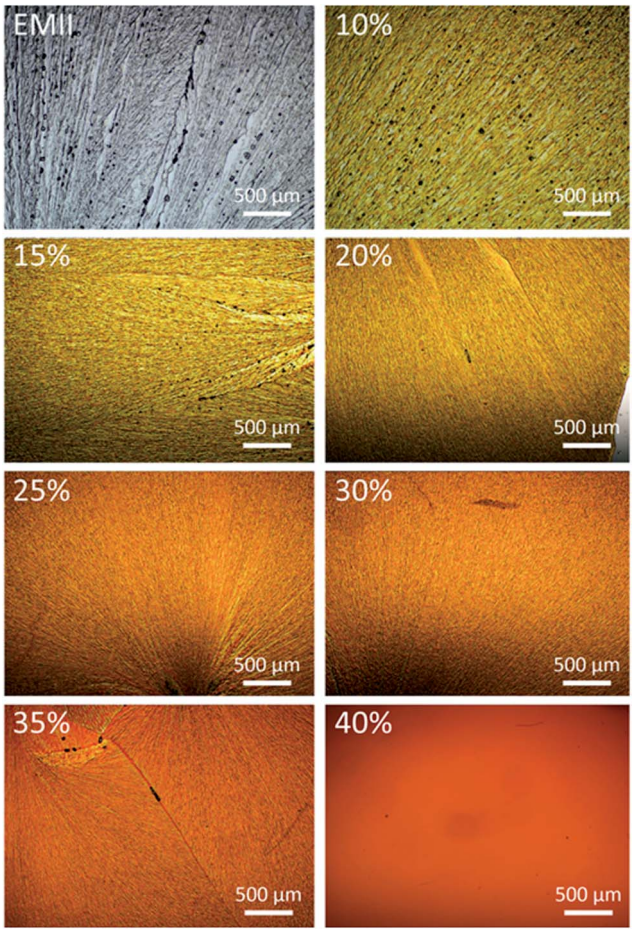

Fig. 3 Optical micrographs of EMII before and after addition of a PMII–iodine mixture (the same molar ratio of 24/1) with increasing the weight percentage from 10% to 40%. The numbers in the top left corners correspond to the weight percentage.

The conductivity of pure EMII was unsatisfactory for the restricted ion diffusion, but PMII exhibited a high conductivity. The conductivity of eutectic melts increased with the addition of the PMII–iodine mixtures. Fig. S2† shows that the conductivity of eutectic melts was elevated by appropriately two times when adding 35 wt% of the PMII–iodine.

To fabricate wire-shaped DSCs, titanium wires were first grown with a layer of aligned titania nanotubes on the surface by an electrochemical anodization method. The titania nanotubes were grown perpendicularly to the Ti surface (Fig. S3†), and their lengths can be controlled by varying the growth time.[23] In this study, titanium wires were modified with 30 μm titania nanotubes (grown in 6 hours). The titania nanotube-modified Ti wire was immersed into N719 solution for dye absorption and used as the working electrode in DSCs. The counter electrode fiber such as the Pt wire was twisted onto the working electrode (Fig. 4a). The other fibers, like bare CNT and the CNT/Pt composite fibers, were also employed as counter electrodes (Fig. S4†). The eutectic melts were heated to 120 °C to form a melt and injected into a fluorine-doped ethylene propylene copolymer tube that was transparent and flexible. The electrolyte was maintained at 80 °C on a heating stage, and the intertwined two fiber electrodes were inserted through the transparent fluorinated ethylene propylene (FEP) tube, followed by sealing at two ends with an ultraviolet curing adhesive. The eutectic melts were infiltrated between the working and counter electrodes (Fig. 4b–d).

The photoelectric performances of the wire-shaped DSCs based on the eutectic melts with different weight percentages of PMII–iodine as electrolytes are shown in Fig. 5. When a DSC is illuminated, the dye (N719) molecule harvests photons and gets excited. The excited dye molecules liberate electrons and inject them to the conducting band of TiO_2, then electrons are transferred to the working electrode and go through the out circuit succeedingly, leaving a hole in the dye (in other words, the dye is oxidized). Then the dye cations capture electrons from

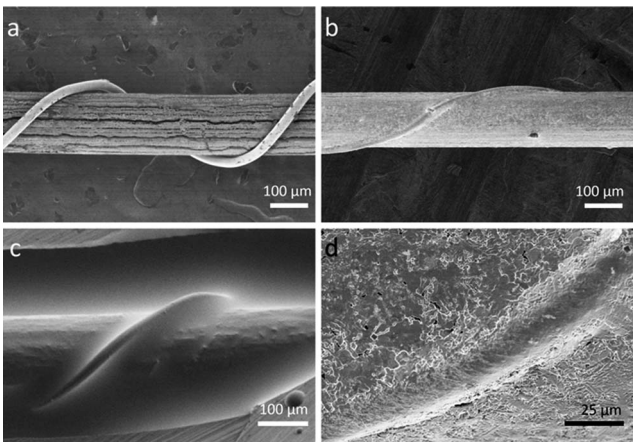

Fig. 4 SEM images of the wire-shaped DSC. (a) Without electrolyte. (b–d) After incorporation of the eutectic melts at different magnifications. Pt wire with a diameter of 25 μm was employed as the counter electrode.

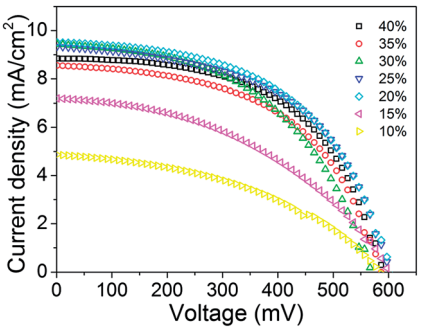

Fig. 5 *J–V* curves of wire-shaped DSCs with increasing PMII–iodine mixture weight percentages from 10% to 40% in eutectic melts. Pt wire with a diameter of 25 μm was employed as the counter electrode to perform these tests.

the I^- anions, oxidizing the I^- anions into I_3^- anions, and the dye is regenerated.

$$2dye^+ + 3I^- \rightarrow 2dye + I_3^- \quad (1)$$

Afterwards, the I_3^- anions diffuse to the counter electrode and obtain electrons from the counter electrode, reducing into I^- anions.

$$I_3^- + 2e \xrightarrow{\text{Pt or CNT}} 3I^- \quad (2)$$

Considering the above mentioned mechanism, the concentration of I^- anions will be a major determinant for the regeneration of N719 dye. Before the concentration of the redox couple reaches a critical value for full regeneration of the dye molecules, the J_{SC} will increase with the increasing proportion of I^-/I_3^- anions. Above the critical value, the amount of I^- anions is adequate to regenerate the dye molecules. However, the light absorption of iodine diminishes the illumination intensity, leading to the decline of J_{SC}, as shown in Fig. 5.

The energy conversion efficiencies were first increased with the increasing PMII–iodine weight percentage from 10% to 20%, since the conductivities were improved. With the further increase of the weight percentage to 40%, the energy conversion efficiencies were gradually decreased as a result of more light absorption of the iodine. The maximal energy conversion efficiency of 3.51% appeared at the PMII–iodine weight percentage of 20% with the open-circuit voltage of 606 mV, short-circuit current density of 9.51 mA cm^{-2} and fill factor of 60.9%.

It should be noted that the cells based on eutectic melts show a relatively lower V_{OC} compared with the acetone-based electrolyte due to their different energy levels caused by different I^-/I_3^- ratios. According to the Nernst equation, the energy level of the I^-/I_3^- redox couple may be changed by varying the concentration ratio of the I^- and I_3^- anions:

$$E = E^0 + \frac{RT}{nF} \ln \frac{[Ox]}{[Red]} \quad (3)$$

where E^0, R, T, n, and F correspond to the standard half-cell reduction potential of I^-/I_3^-, ideal gas constant, temperature in

the Kelvin scale, mole of electrons transferred in the cell reaction or half-reaction and Faraday constant. In the case of DSCs, there was a trade-off between J_{SC} and V_{OC}. A lower PMII–iodine ratio caused a positive shift in the redox potential of the electrolyte,[24] leading to a lower V_{OC} but higher J_{SC}. The ratio of 24/1 was found to achieve the highest efficiency, similar to the other reports to maximize the efficiency through a trade-off between V_{OC} and J_{SC}.[25,26] In addition, the energy conversion efficiencies could also be improved by fabricating the wire-shaped DSC on different substrates, *e.g.*, 4.22% and 4.67% on mirror and paper, respectively (Fig. S5†).

To elucidate the obtained short-circuit current density in the wire-shaped DSC, the incident photon-to-electron conversion efficiency (IPCE) of the device using electrolyte with 20 wt% PMII–iodine was measured as a function of the wavelength (Fig. S6†). A maximum of ~75% was obtained at a wavelength of 530 nm. Note that the eutectic melts were also applicable to the other fiber electrodes, apart from Pt wires, such as CNT fibers and CNT/Pt composite fibers (Fig. S7 and S8†).

Although the energy conversion efficiency is relatively lower than 6.58% for the case of a liquid electrolyte (Fig. S9†), Fig. 6 implies that the stability of a DSC with eutectic melts is much higher than that of a liquid electrolyte. Fermi levels of the photovoltaic materials were clearly changed under heating, correspondingly, the open-circuit voltages rapidly declined when heated from 30 to 110 °C (Fig. 6a). However, the diffusion of ions in electrolytes was enhanced at higher temperatures to increase the short-circuit current densities (Fig. 6b). Overall, the energy conversion efficiencies typically decreased with the increasing temperature (Fig. 6c). The above phenomena were consistent for both liquid electrolytes and eutectic melts in the wire-shaped DSC. However, for the liquid electrolyte containing organic solvent, like acetonitrile, that may be vaporized and leaked during heating, particularly above the boiling point, the energy conversion efficiencies cannot revert to the original values after cooling down to low temperatures. In other words, the wire-shaped DSCs based on the liquid electrolyte cannot be effectively used at high temperatures. In contrast, the efficiency derived from the eutectic melts was entirely recovered after heating up to 100 °C and then cooling down to 30 °C. Fig. 6d further shows that the wire-shaped DSC based on the eutectic melts can be stably operated after repeated heating and cooling for many cycles. In stark contrast, the wire-shaped DSC based on the conventional liquid electrolyte reluctantly maintained the energy conversion efficiency by less than 10% after only two cycles.

As for the wire-shaped DSCs based on the eutectic melts and liquid electrolytes, the efficiency evolution was traced respectively over a period of 30 days under the same conditions (Fig. 7). For the eutectic melts, the solar cell maintained an energy conversion efficiency of 90%, while for the liquid electrolyte, only 8% remained. It should be noticed that these tests were carried out using cells with makeshift encapsulation, similar to other published work.[6] The electrolyte would corrode the adhesives in the ends of the encapsulation tube, resulting in pinholes where solvents of electrolyte may leak, which would lead to a quick failure of conventional liquid electrolyte DSCs. In addition, the wire-shaped DSCs based on the eutectic melts were also flexible. Fig. 8 shows that the energy conversion efficiencies were well maintained at a bending curvature of 3.3 cm^{-1}.

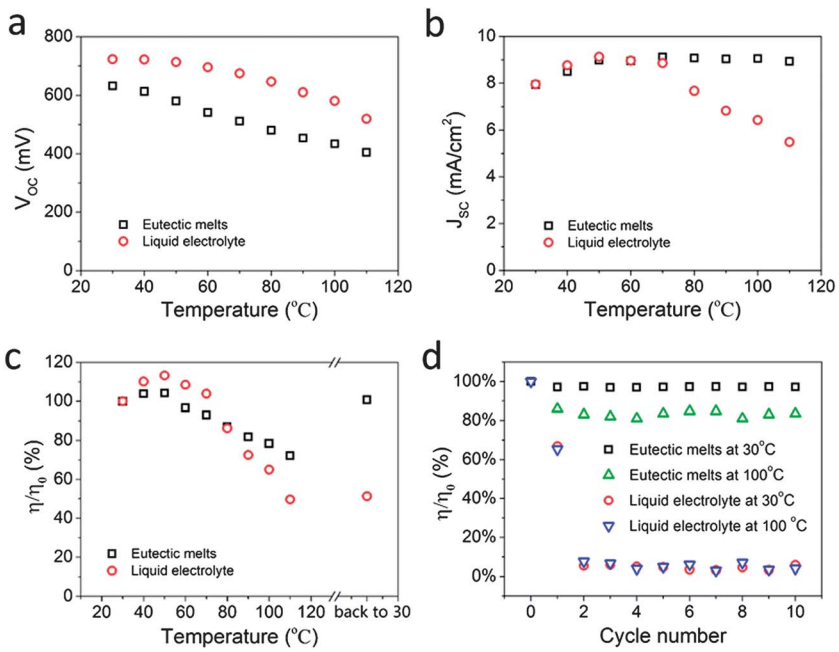

Fig. 6 A comparison of the thermal stability of the wire-shaped DSCs based on liquid electrolyte and the eutectic melts electrolyte with 20 wt% PMII–iodine (molar ratio of PMII and iodine, 24/1). (a–c). Dependence of V_{OC}, J_{SC}, and η/η_0 on the temperature, respectively. (d) η/η_0 values at 30 °C and 100 °C. The wire-shaped DSCs were repeatedly heated to 100 °C and then cooled down to 30 °C. η and η_0 correspond to the energy conversion efficiencies of the as-fabricated wire-shaped DSC and the one after heating treatment. Pt wire with a diameter of 25 μm was employed as the counter electrode to perform these tests.

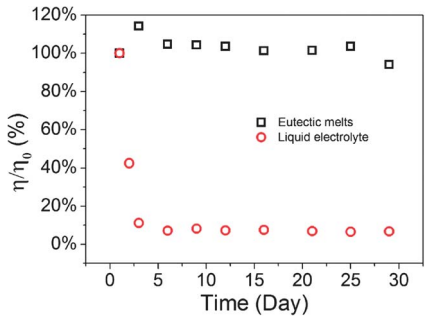

Fig. 7 Comparison of the operation stability of the wire-shaped DSCs based on liquid electrolyte and eutectic melts. η and η_0 correspond to the energy conversion efficiencies of the as-fabricated wire-shaped DSCs and the one at the corresponding time during use. The devices were kept in the dark in a temperature range of (25 ± 5) °C and humidity range of (40 ± 30)%.

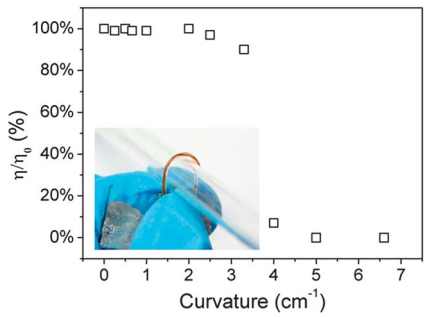

Fig. 8 Flexibility of the wire-shaped DSC by tracing the energy conversion efficiency under bending with increasing curvature. Here η_0 and η correspond to the energy conversion efficiencies before and after deformation, respectively. The inserted image shows a typical photograph of the bending. Eutectic melts with 20 wt% PMII–iodine (molar ratio of PMII and iodine, 24/1) and a Pt wire counter electrode was used.

Conclusion

In summary, eutectic melts, for the first time, were used to develop novel wire-shaped dye-sensitized solar cells that are flexible and thermally stable even at a high temperature of 110 °C. They were shown to be well applicable to a wide variety of fiber-like counter electrodes and represent a general approach to enhance the high performance optoelectronic devices. More efforts are underway to further improve their energy conversion efficiencies and integrate them into deformable electronic textiles.

Acknowledgements

This work was supported by the NSFC (21225417), MOST (2011CB932503), STCSM (12nm0503200), Fok Ying Tong Education Foundation, The Program for Professor of Special Appointment at Shanghai Institutions of Higher Learning, and the Program for Outstanding Young Scholars from Organization Department of the CPC Central Committee. The authors also want to thank B. Zhang and Z. Chen for their help with the thermal analysis.

References

1 P. V. Kamat, *J. Phys. Chem. C*, 2007, **111**, 2834–2860.
2 M. Gratzel, *J. Photochem. Photobiol., C*, 2003, **4**, 145–153.
3 T. Chen, L. Qiu, Z. Yang and H. Peng, *Chem. Soc. Rev.*, 2013, **42**, 5031–5041.
4 X. Fan, Z. Z. Chu, F. Z. Wang, C. Zhang, L. Chen, Y. W. Tang and D. C. Zou, *Adv. Mater.*, 2008, **20**, 592–595.
5 D. Liu, M. Zhao, Y. Li, Z. Bian, L. Zhang, Y. Shang, X. Xia, S. Zhang, D. Yun, Z. Liu, A. Cao and C. Huang, *ACS Nano*, 2012, **6**, 11027–11034.
6 Z. Lv, Y. Fu, S. Hou, D. Wang, H. Wu, C. Zhang, Z. Chu and D. Zou, *Phys. Chem. Chem. Phys.*, 2011, **13**, 10076–10083.
7 T. Chen, L. Qiu, Z. Cai, F. Gong, Z. Yang, Z. Wang and H. Peng, *Nano Lett.*, 2012, **12**, 2568–2572.
8 S. Huang, X. Guo, X. Huang, Q. Zhang, H. Sun, D. Li, Y. Luo and Q. Meng, *Nanotechnology*, 2011, **22**, 315402.
9 Z. Yang, H. Sun, T. Chen, L. Qiu, Y. Luo and H. Peng, *Angew. Chem., Int. Ed.*, 2013, **52**, 7545–7548.
10 D. Li, D. Qin, M. Deng, Y. Luo and Q. Meng, *Energy Environ. Sci.*, 2009, **2**, 283–291.
11 R. D. Rogers and K. R. Seddon, *Science*, 2003, **302**, 792–793.
12 P. Wang, S. M. Zakeeruddin, P. Comte, I. Exnar and M. Grätzel, *J. Am. Chem. Soc.*, 2003, **125**, 1166–1167.
13 L. J. Brennan, S. Barwich, A. Satti and Y. Gunko, *J. Mater. Chem. A*, 2013, **1**, 8379–8384.
14 I. J. Lin and C. S. Vasam, *J. Organomet. Chem.*, 2005, **690**, 3498–3512.
15 D. Kuang, P. Wang, S. Ito, S. M. Zakeeruddin and M. Grätzel, *J. Am. Chem. Soc.*, 2006, **128**, 7732–7733.
16 L. V. N. R. Ganapatibhotla, J. Zheng, D. Roy and S. Krishnan, *Chem. Mater.*, 2010, **22**, 6347–6360.
17 E. Guillén, C. Fernández-Lorenzo, R. Alcántara, J. Martín-Calleja and J. A. Anta, *Sol. Energy Mater. Sol. Cells*, 2009, **93**, 1846–1852.
18 Y. Bai, Y. Cao, J. Zhang, M. Wang, R. Li, P. Wang, S. M. Zakeeruddin and M. Grätzel, *Nat. Mater.*, 2008, **7**, 626–630.
19 K. Jiang, Q. Li and S. Fan, *Nature*, 2002, **419**, 801–801.
20 H. Sun, Z. Yang, X. Chen, L. Qiu, X. You, P. Chen and H. Peng, *Angew. Chem., Int. Ed.*, 2013, **52**, 8276–8280.
21 S. Pan, Z. Yang, H. Li, L. Qiu, H. Sun and H. Peng, *J. Am. Chem. Soc.*, 2013, **135**, 10622–10625.
22 Q. Zhang, D. Myers, J. Lan, S. A. Jenekhe and G. Cao, *Phys. Chem. Chem. Phys.*, 2012, **14**, 14982–14998.
23 T. Chen, L. Qiu, H. G. Kia, Z. Yang and H. Peng, *Adv. Mater.*, 2012, **24**, 4623–4628.
24 Z. Yu, M. Gorlov, J. Nissfolk, G. Boschloo and L. Kloo, *J. Phys. Chem. C*, 2010, **114**, 10612–10620.
25 H. Wang, X. Zhang, F. Gong, G. Zhou and Z. S. Wang, *Adv. Mater.*, 2012, **24**, 121–124.
26 Q. Li, J. Zhao, B. Sun, B. Lin, L. Qiu, Y. Zhang, X. Chen, J. Lu and F. Yan, *Adv. Mater.*, 2012, **24**, 945–950.